

## SUPERCONVERGENCE OF DG METHOD FOR ONE-DIMENSIONAL SINGULARLY PERTURBED PROBLEMS <sup>\*1)</sup>

Ziqing Xie

*(College of Mathematics and Computer Science, Hunan Normal University, Changsha 410081, China  
Email: ziqingxie@hunnu.edu.cn)*

Zhimin Zhang

*(College of Mathematics and Computer Science, Hunan Normal University, Changsha 410081, China  
Department of Mathematics, Wayne State University, Detroit, MI 48202, USA  
Email: zzhang@math.wayne.edu)*

### Abstract

The convergence and superconvergence properties of the discontinuous Galerkin (DG) method for a singularly perturbed model problem in one-dimensional setting are studied. By applying the DG method with appropriately chosen numerical traces, the existence and uniqueness of the DG solution, the optimal order  $L_2$  error bounds, and  $2p + 1$ -order superconvergence of the numerical traces are established. The numerical results indicate that the DG method does not produce any oscillation even under the uniform mesh. Numerical experiments demonstrate that, under the uniform mesh, it seems impossible to obtain the uniform superconvergence of the numerical traces. Nevertheless, thanks to the implementation of the so-called Shishkin-type mesh, the uniform  $2p + 1$ -order superconvergence is observed numerically.

*Mathematics subject classification:* 65N30.

*Key words:* Discontinuous Galerkin methods, Singular perturbation, Superconvergence, Shishkin mesh, Numerical traces.

## 1. Introduction

In scientific and engineering computation, we often encounter differential equations with small parameters and these equations are “singularly perturbed”. One of the difficulties in numerically computing the solution of singularly perturbed problems lays in the so-called boundary layer behavior, i.e., the solution varies very rapidly in a very thin layer near the boundary. Traditional methods, such as finite element and finite difference methods, do not work well for these problems as they often produce oscillatory solutions which are inaccurate when the diffusion parameter is small. Numerical simulations of these equations raise very challenging problems for scientists and engineers. There is a rich literature in this direction. The reader is referred to books [14, 15, 18] and survey articles [17, 22] for details. Currently, this is still a very active field, see, e.g., [6, 10, 13, 19]. We have also noticed some publications in this journal on the topic, see, e.g., [12], among others.

---

\* Received April 15, 2005; final revised November 2, 2006; accepted December 5, 2006.

<sup>1)</sup> This work is supported in part by the National Natural Science Foundation of China (10571053), Program for New Century Excellent Talents in University, and the Scientific Research Fund of Hunan Provincial Education Department (0513039). The second author is supported in part by the US National Science Foundation under grants DMS-0311807 and DMS-0612908.

Since the introduction of the first DG method for hyperbolic equations [16], there has been an active development of DG methods for hyperbolic and elliptic equations in parallel, e.g., [1, 7, 8], some recent development [2, 24], and references therein. The model problem in this article is a singularly perturbed convection-diffusion equation in the one-dimensional setting. When the small parameter approaches 0, the problem changes from an elliptic equation to a hyperbolic equation. The superconvergence property of the traditional finite element method under the Shishkin mesh [20] for this model problem was discussed in [26], and the p-version finite element method for this model problem was studied in [21, 25] among others. Inspired by the great success of the DG method in solving hyperbolic equations [7], we adopt it to solve the singularly perturbed convection-diffusion equations.

In this work, we first define the DG scheme by choosing the numerical trace which is very delicate as it can affect the stability and accuracy. Next we verify the existence and uniqueness of the approximate solution. We then focus on the proof of  $2p + 1$ -order superconvergence of the numerical traces at the nodes. For arbitrary  $\epsilon$ , the uniform convergence is expected. The so-called “uniform convergence” means that the convergence rate is uniformly valid in terms of the singular perturbation parameter  $\epsilon$ . The numerical results in Section 3 indicate that, under the uniform mesh, it seems impossible to have the uniform  $2p + 1$ -order superconvergence. Nevertheless, an attractive feature is that the DG method does not produce any oscillation outside boundary region even under the uniform mesh. In other words, the DG method is more “local” than the traditional finite element method. On the other hand, when the Shishkin-type meshes are implemented with some appropriately chosen  $\tau$ , the length of the boundary layer in numerical computation, the uniform superconvergent results are observed in our numerical experiments in Section 3. The theoretical analysis of this exciting phenomenon is an ongoing work. Further, the approach in this work can be generalized to the two-dimensional setting.

During the process of this study, we noticed a parallel work [3], which addressed the same superconvergence issue for the model problem. However, two approaches are completely different and our proof is much simpler. As for general finite element superconvergence theory, we refer readers to following books [4, 5, 9, 11, 23, 27] and references therein.

## 2. DG Method

Consider the following one-dimensional convection-diffusion problem,

$$\begin{cases} -\epsilon u'' + bu' = f & \text{in } (0, 1), \\ u(0) = u_0, \quad u'(1) = u'_1, \end{cases} \quad (2.1)$$

where  $b > 0$  and  $\epsilon$  is a small positive parameter. The choice of  $b > 0$  guarantees that the location of the possible boundary layer is at the outflow boundary  $x = 1$ .

By setting  $q = u'$ , (2.1) can be rewritten as

$$\begin{cases} -\epsilon q' + bq = f & \text{in } (0, 1), \\ q - u' = 0, \\ u(0) = u_0, \quad q(1) = u'_1. \end{cases} \quad (2.2)$$

Denote the mesh by  $I_j = [x_{j-\frac{1}{2}}, x_{j+\frac{1}{2}}]$  for  $j = 1, \dots, N$  with  $x_{\frac{1}{2}} = 0, x_{N+\frac{1}{2}} = 1$ . The center of the cell  $I_j$  is  $x_j = (x_{j-\frac{1}{2}} + x_{j+\frac{1}{2}})/2$  and  $h_j = |I_j|$ . Set  $h = \max_{1 \leq j \leq N} h_j$  and  $\Omega_h = \bigcup_{j=1}^N I_j$ . We denote by  $u_{j+\frac{1}{2}}^+$  and  $u_{j+\frac{1}{2}}^-$  the values of  $u$  at  $x_{j+\frac{1}{2}}$ , from the right cell and the left cell of  $x_{j+\frac{1}{2}}$ , respectively. Denote the jump at  $x_{j+\frac{1}{2}}$  by  $[u]_{j+\frac{1}{2}} = u_{j+\frac{1}{2}}^+ - u_{j+\frac{1}{2}}^-$ .

We multiply the two equations of (2.2) by test functions  $v$  and  $w$ , respectively, and integrate by parts in each cell  $I_j$  to obtain,

$$\begin{aligned} \epsilon \int_{I_j} qv'dx + b \int_{I_j} qvdx - \epsilon q_{j+\frac{1}{2}}^- v_{j+\frac{1}{2}}^- + \epsilon q_{j-\frac{1}{2}}^+ v_{j-\frac{1}{2}}^+ &= \int_{I_j} fvd x, \quad 1 \leq j \leq N, \\ \int_{I_j} uw'dx + \int_{I_j} qw dx - u_{j+\frac{1}{2}}^- w_{j+\frac{1}{2}}^- + u_{j-\frac{1}{2}}^+ w_{j-\frac{1}{2}}^+ &= 0, \quad 1 \leq j \leq N. \end{aligned}$$

This is the weak formulation we shall use to define the DG methods.

Now define the piecewise polynomial space  $V_h$  as the space of polynomials of degree  $p \geq 1$  in each cell  $I_j$ , i.e.,

$$V_h = \{v : v \in P_p(I_j), \quad j = 1, \dots, N\}.$$

Moreover, define the space

$$H^k(\Omega_h) = \{v : v \in H^k(I_j), \quad j = 1, \dots, N\}$$

with  $k \geq 0$ . We will search for approximate solutions of (2.2) in terms of piecewise polynomial functions  $U, Q \in V_h$  that satisfy (2.2) in a weak sense. Following Cockburn and Shu [8], we consider the following general formulation: Find  $U, Q \in V_h$  such that

$$\epsilon \int_{I_j} Qv'dx + b \int_{I_j} Qvdx - \epsilon \hat{Q}_{j+\frac{1}{2}} v_{j+\frac{1}{2}}^- + \epsilon \hat{Q}_{j-\frac{1}{2}} v_{j-\frac{1}{2}}^+ = \int_{I_j} fvd x, \quad (2.3)$$

$$\int_{I_j} Uv'dx + \int_{I_j} Qvdx - \hat{U}_{j+\frac{1}{2}} v_{j+\frac{1}{2}}^- + \hat{U}_{j-\frac{1}{2}} v_{j-\frac{1}{2}}^+ = 0 \quad (2.4)$$

for any  $v$  and  $w \in V_h$ . To complete the specification of a DG method, one must define the numerical traces  $\hat{U}$  and  $\hat{Q}$  at the nodes. Through the specification of the numerical traces, the interaction of  $U$  and  $Q$  in different intervals  $I_j$  and the boundary conditions are imposed. The impact of the choice of the numerical traces on the DG method for solving the linear elliptic equation was shown in [1].

In this article, we take the following numerical traces:

$$\hat{U}_{j+\frac{1}{2}} = \begin{cases} u_0 & j = 0, \\ U_{j+\frac{1}{2}}^- & j = 1, \dots, N, \end{cases} \quad (2.5)$$

$$\hat{Q}_{j+\frac{1}{2}} = \begin{cases} Q_{j+\frac{1}{2}}^+ & j = 0, 1, \dots, N-1, \\ u_1' & j = N. \end{cases} \quad (2.6)$$

The following theorem guarantees the existence and uniqueness of the numerical solution defined by (2.3)-(2.6).

**Theorem 2.1.** *The DG method defined by (2.3), (2.4) with the numerical traces (2.5) and (2.6) has a unique solution.*

*Proof.* Integrated by parts, (2.3) and (2.4) can be rewritten as

$$\int_{I_j} (-\epsilon Q' + bQ)vdx - \epsilon [Q]_{j+\frac{1}{2}} v_{j+\frac{1}{2}}^- = \int_{I_j} fvd x, \quad (2.7)$$

$$\int_{I_j} (-U' + Q)w dx - [U]_{j-\frac{1}{2}} w_{j-\frac{1}{2}}^+ = 0, \quad (2.8)$$

respectively. Summing up (2.3) and (2.7), respectively, we obtain

$$\sum_{j=1}^N \int_{I_j} (\epsilon Qv' + bQv)dx - \epsilon \hat{Q}_{N+\frac{1}{2}} v_{N+\frac{1}{2}}^- + \epsilon \hat{Q}_{\frac{1}{2}} v_{\frac{1}{2}}^+ + \epsilon \sum_{j=1}^{N-1} \hat{Q}_{j+\frac{1}{2}} [v]_{j+\frac{1}{2}} = \sum_{j=1}^N \int_{I_j} fvd x, \quad (2.9)$$

$$\sum_{j=1}^N \int_{I_j} (-\epsilon Q' + bQ)vdx - \epsilon \sum_{j=1}^{N-1} [Q]_{j+\frac{1}{2}} v_{j+\frac{1}{2}}^- - \epsilon [Q]_{N+\frac{1}{2}} v_{N+\frac{1}{2}}^- = \sum_{j=1}^N \int_{I_j} fvd x. \quad (2.10)$$

Adding (2.9) and (2.10) with  $v = Q$ , we have

$$\begin{aligned} & 2b \sum_{j=1}^N \int_{I_j} Q^2 dx + \epsilon (\hat{Q}_{\frac{1}{2}})^2 + \epsilon \sum_{j=1}^{N-1} [Q]_{j+\frac{1}{2}}^2 - 2\epsilon \hat{Q}_{N+\frac{1}{2}} Q_{N+\frac{1}{2}}^- + \epsilon (Q_{N+\frac{1}{2}}^-)^2 \quad (2.11) \\ & = 2 \sum_{j=1}^N \int_{I_j} f Q dx, \end{aligned}$$

where the numerical trace  $\hat{Q}$  in (2.6) is used.

Now summing up (2.4) and (2.8), respectively, we have

$$\sum_{j=1}^N \int_{I_j} (U w' + Q w) dx - \hat{U}_{N+\frac{1}{2}} w_{N+\frac{1}{2}}^- + \hat{U}_{\frac{1}{2}} w_{\frac{1}{2}}^+ + \sum_{j=1}^{N-1} \hat{U}_{j+\frac{1}{2}} [w]_{j+\frac{1}{2}} = 0, \quad (2.12)$$

$$\sum_{j=1}^N \int_{I_j} (-U' + Q) w dx - \sum_{j=1}^{N-1} [U]_{j+\frac{1}{2}} w_{j+\frac{1}{2}}^+ - [U]_{\frac{1}{2}} w_{\frac{1}{2}}^+ = 0. \quad (2.13)$$

Adding (2.12) and (2.13) with  $w = U$ , we have

$$2 \sum_{j=1}^N \int_{I_j} Q U dx - \sum_{j=1}^{N-1} ([U]_{j+\frac{1}{2}})^2 - (U_{\frac{1}{2}}^+)^2 - (\hat{U}_{N+\frac{1}{2}})^2 + 2\hat{U}_{\frac{1}{2}} U_{\frac{1}{2}}^+ = 0. \quad (2.14)$$

Due to the linearity and finite dimensionality of the problem, to prove this theorem, it is sufficient to verify that the only solution to (2.3)-(2.6) with  $f = 0$ ,  $u_0 = 0$  and  $u_1' = 0$  is  $U = 0$  and  $Q = 0$ . By (2.11),

$$2b \sum_{j=1}^N \int_{I_j} Q^2 dx + \epsilon (\hat{Q}_{\frac{1}{2}})^2 + \epsilon \sum_{j=1}^{N-1} [Q]_{j+\frac{1}{2}}^2 + \epsilon (Q_{N+\frac{1}{2}}^-)^2 = 0. \quad (2.15)$$

If  $b \neq 0$ , (2.15) implies  $Q = 0$ . If  $b = 0$ , (2.15) implies

$$\hat{Q}_{\frac{1}{2}} = 0, \quad Q_{N+\frac{1}{2}}^- = 0, \quad [Q]_{j+\frac{1}{2}} = 0, \quad \text{for } j = 1, \dots, N-1.$$

This, combining with (2.10), implies that

$$\sum_{j=1}^N \int_{I_j} Q' v dx = 0, \quad \forall v \in V_h,$$

which results in  $Q' = 0$ . As a result,  $Q$  is piecewise constant. Due to  $Q_{N+\frac{1}{2}}^- = 0$  and  $[Q]_{j+\frac{1}{2}} = 0$ , for  $j = 1, \dots, N-1$ , we have  $Q = 0$ .

On the other hand, from (2.14), we know

$$U_{\frac{1}{2}}^+ = 0, \quad \hat{U}_{N+\frac{1}{2}} = 0, \quad [U]_{j+\frac{1}{2}} = 0 \quad \text{for } j = 1, \dots, N-1.$$

This, combining with (2.13), implies that

$$\sum_{j=1}^N \int_{I_j} U' w dx = 0, \quad \forall w \in V_h,$$

which implies  $U = 0$ .

### 3. Superconvergence of the Numerical Traces

Now we turn to investigate superconvergence properties of the numerical traces at nodes. Note that the scheme (2.3) and (2.4) with (2.5) and (2.6) are consistent, i.e., the exact solutions

$q$  and  $u$  of (2.2) also satisfy (2.3) and (2.4). Denote the errors by  $e_q = q - Q$  and  $e_u = u - U$ . To simplify notations, we set

$$B_1^{(j)}(q; v) = \epsilon \int_{I_j} qv' dx + b \int_{I_j} qv dx - \epsilon \hat{q}_{j+\frac{1}{2}} v_{j+\frac{1}{2}}^- + \epsilon \hat{q}_{j-\frac{1}{2}} v_{j-\frac{1}{2}}^+, \quad (3.1)$$

$$B_2^{(j)}(q, u; w) = \int_{I_j} uw' dx + \int_{I_j} qw dx - \hat{u}_{j+\frac{1}{2}} w_{j+\frac{1}{2}}^- + \hat{u}_{j-\frac{1}{2}} w_{j-\frac{1}{2}}^+. \quad (3.2)$$

Then  $e_q$  and  $e_u$  satisfy the error equations

$$B_1^{(j)}(e_q; v) = 0, \quad B_2^{(j)}(e_q, e_u; w) = 0, \quad \forall v, w \in V_h. \quad (3.3)$$

Set

$$B^{(j)}(q, u; v, w) = B_1^{(j)}(q; v) + B_2^{(j)}(q, u; w).$$

By (3.1) and (3.2),

$$\begin{aligned} B^{(j)}(q, u; v, w) &= \int_{I_j} (\epsilon v' + bv + w)q dx + \int_{I_j} w' u dx \\ &\quad - \epsilon \hat{q}_{j+\frac{1}{2}} v_{j+\frac{1}{2}}^- + \epsilon \hat{q}_{j-\frac{1}{2}} v_{j-\frac{1}{2}}^+ - \hat{u}_{j+\frac{1}{2}} w_{j+\frac{1}{2}}^- + \hat{u}_{j-\frac{1}{2}} w_{j-\frac{1}{2}}^+. \end{aligned} \quad (3.4)$$

By (3.3), we have

$$B^{(j)}(e_q, e_u; v, w) = 0, \quad \forall v, w \in V_h. \quad (3.5)$$

Integrated by parts in (3.1) and (3.2) and in terms of the numerical traces (2.5) and (2.6),  $B_1^{(j)}(q; v)$  and  $B_2^{(j)}(q, u; w)$  can be rewritten as

$$B_1^{(j)}(q; v) = \int_{I_j} (-\epsilon q' + bq)v dx - \epsilon [q]_{j+\frac{1}{2}} v_{j+\frac{1}{2}}^-, \quad (3.6)$$

$$B_2^{(j)}(q, u; w) = \int_{I_j} (-u' + q)w dx - [u]_{j-\frac{1}{2}} w_{j-\frac{1}{2}}^+. \quad (3.7)$$

Hence  $B^{(j)}(q, u; v, w)$  can also be written as

$$\begin{aligned} &B^{(j)}(q, u; v, w) \\ &= \int_{I_j} (-\epsilon q' + bq)v dx + \int_{I_j} (-u' + q)w dx - \epsilon [q]_{j+\frac{1}{2}} v_{j+\frac{1}{2}}^- - [u]_{j-\frac{1}{2}} w_{j-\frac{1}{2}}^+. \end{aligned} \quad (3.8)$$

For convenience, let us introduce the p-degree projection operator  $\pi^\pm$  as follows. For  $\forall u \in H^1(\Omega_h)$ ,

$$\begin{aligned} (\phi - \pi^- \phi)_{j+\frac{1}{2}}^- &= 0, \quad \int_{I_j} (\phi - \pi^- \phi)v = 0, \quad \forall v \in P_{p-1}(I_j), \\ (\phi - \pi^+ \phi)_{j-\frac{1}{2}}^+ &= 0, \quad \int_{I_j} (\phi - \pi^+ \phi)v = 0, \quad \forall v \in P_{p-1}(I_j), \end{aligned}$$

and  $\pi^\pm u \in V_h$ . The existence of the above projection operators and the corresponding approximation results can be seen in [4]. We just quote those estimates from [4] directly.

**Lemma 3.1.** For  $u \in H^{p+1}(I_j)$  with  $j = 1, \dots, N$ , the following results hold:

$$\|D^\alpha(u - \pi^\pm u)\|_{I_j} \leq Ch^{p+1-\alpha} |u|_{p+1, I_j}, \quad \alpha = 0, 1.$$

**Theorem 3.1.** Consider the DG method defined by the weak form (2.3) and (2.4) with the numerical traces (2.5) and (2.6). Suppose  $u \in H^{p+2}(\Omega_h)$  for some  $p \geq 1$ . Then

$$\|e_u\| \leq C(\epsilon)h^{p+1} \|u\|_{p+2}, \quad \|e_q\| \leq C(\epsilon)h^{p+1} \|u\|_{p+2}.$$

*Proof.* We construct an adjoint problem,

$$\begin{cases} \epsilon V' + bV + W = e_q & \text{in } (0, 1), \\ W' = e_u, \\ V(0) = 0, \quad W(1) = 0, \end{cases} \quad (3.9)$$

which has the solution

$$W(x) = - \int_x^1 e_u dx, \quad V(x) = \frac{1}{\epsilon} e^{-\frac{bx}{\epsilon}} \int_0^x (e_q - W) e^{\frac{bt}{\epsilon}} dt. \quad (3.10)$$

By (3.4) and (3.9), we have

$$\begin{aligned} & B^{(j)}(e_q, e_u; V, W) \\ &= \int_{I_j} (\epsilon V' + bV + W) e_q dx + \int_{I_j} W' e_u dx \\ & \quad - \epsilon (\hat{e}_q)_{j+\frac{1}{2}} V_{j+\frac{1}{2}}^- + \epsilon (\hat{e}_q)_{j-\frac{1}{2}} V_{j-\frac{1}{2}}^+ - (\hat{e}_u)_{j+\frac{1}{2}} W_{j+\frac{1}{2}}^- + (\hat{e}_u)_{j-\frac{1}{2}} W_{j-\frac{1}{2}}^+ \\ &= \int_{I_j} e_q^2 dx + \int_{I_j} e_u^2 dx - \epsilon (\hat{e}_q)_{j+\frac{1}{2}} V_{j+\frac{1}{2}}^- + \epsilon (\hat{e}_q)_{j-\frac{1}{2}} V_{j-\frac{1}{2}}^+ - (\hat{e}_u)_{j+\frac{1}{2}} W_{j+\frac{1}{2}}^- + (\hat{e}_u)_{j-\frac{1}{2}} W_{j-\frac{1}{2}}^+. \end{aligned} \quad (3.11)$$

Summing up, we have

$$\begin{aligned} & \sum_{j=1}^N B^{(j)}(e_q, e_u; V, W) \\ &= \|e_q\|^2 + \|e_u\|^2 - \epsilon (\hat{e}_q)_{N+\frac{1}{2}} V_{N+\frac{1}{2}}^- + \epsilon (\hat{e}_q)_{\frac{1}{2}} (V)_{\frac{1}{2}}^+ - (\hat{e}_u)_{N+\frac{1}{2}} (W)_{N+\frac{1}{2}}^- + (\hat{e}_u)_{\frac{1}{2}} W_{\frac{1}{2}}^+ \\ &= \|e_q\|^2 + \|e_u\|^2, \end{aligned} \quad (3.12)$$

where  $(\hat{e}_q)_{N+\frac{1}{2}} = 0$ ,  $(\hat{e}_u)_{\frac{1}{2}} = 0$  and the boundary conditions in (3.9) are used.

On the other hand, by (3.8) and (3.5), we have

$$\begin{aligned} & \sum_{j=1}^N B^{(j)}(e_q, e_u; V, W) \\ &= \sum_{j=1}^N B^{(j)}(e_q, e_u; V - \pi^- V, W - \pi^+ W) \\ &= \sum_{j=1}^N \int_{I_j} (-\epsilon e'_q + b e_q)(V - \pi^- V) dx + \int_{I_j} (-e'_u + e_q)(W - \pi^+ W) dx \\ &= \sum_{j=1}^N \int_{I_j} [-\epsilon(q - \pi^- q)' + b e_q](V - \pi^- V) dx + \int_{I_j} [-(u - \pi^+ u)' + e_q](W - \pi^+ W) dx, \end{aligned} \quad (3.13)$$

where the properties of the operators  $\pi^-$  and  $\pi^+$  are used. By (3.12) and (3.13), we have

$$\begin{aligned} & \|e_q\|^2 + \|e_u\|^2 \\ &\leq (\epsilon \|(q - \pi^- q)'\| + \|e_q\|) \|V - \pi^- V\| + (\|(u - \pi^+ u)'\| + \|e_q\|) \|W - \pi^+ W\| \\ &\leq C_0 (C_1 \epsilon h^p |q|_{p+1} + \|e_q\|) h |V|_1 + C_2 (C_3 h^p |u|_{p+1} + \|e_q\|) h |W|_1 \\ &\leq C_0 (C_1 \epsilon h^{p+1} |q|_{p+1} + h \|e_q\|) |V|_1 + C_2 (C_3 h^{p+1} |u|_{p+1} + h \|e_q\|) |W|_1. \end{aligned} \quad (3.14)$$

By (3.10), we obtain

$$|W|_1 = \|e_u\|, \quad |V|_1 \leq C(\epsilon) (\|e_q\| + \|e_u\|).$$

This, combining (3.14), implies that

$$\|e_u\| \leq C(\epsilon) h^{p+1} \|u\|_{p+2}, \quad \|e_q\| \leq C(\epsilon) h^{p+1} \|u\|_{p+2}.$$

Based on the  $L_2$  estimate of the errors, we will investigate the superconvergence properties of the numerical traces in the following theorem.

**Theorem 3.2.** *Under the same assumptions as in Theorem 3.1 with  $b \neq 0$ , we have*

$$\begin{aligned} |(\hat{e}_u)_{n+\frac{1}{2}}| &\leq C(\epsilon)h^{2p+1}\|u\|_{p+2}, \\ |(\hat{e}_q)_{n-\frac{1}{2}}| &\leq C(\epsilon)h^{2p+1}\|u\|_{p+2}, \quad n = 1, \dots, N. \end{aligned}$$

*Proof.* First consider the superconvergence of  $(\hat{e}_q)_{n-\frac{1}{2}}$ . For this purpose, we construct another adjoint problem,

$$\begin{cases} \epsilon V' + bV + W = 0 & \text{in } \Omega_1 = [x_{n-\frac{1}{2}}, 1], \\ W' = 0, \\ V(x_{n-\frac{1}{2}}) = (\hat{e}_q)_{n-\frac{1}{2}}, \quad W(1) = 0. \end{cases} \quad (3.15)$$

A simple calculation shows that (3.15) has the solutions

$$V = (\hat{e}_q)_{n-\frac{1}{2}}e^{b(x_{n-\frac{1}{2}}-x)/\epsilon}, \quad W = 0. \quad (3.16)$$

The combination of (3.4) and (3.15) implies that

$$\begin{aligned} &B^{(j)}(e_q, e_u; V, W) \\ &= \int_{I_j} (\epsilon V' + bV + W)e_q dx + \int_{I_j} W'e_u dx \\ &\quad - \epsilon(\hat{e}_q)_{j+\frac{1}{2}}V_{j+\frac{1}{2}}^- + \epsilon(\hat{e}_q)_{j-\frac{1}{2}}V_{j-\frac{1}{2}}^+ - (\hat{e}_u)_{j+\frac{1}{2}}W_{j+\frac{1}{2}}^- + (\hat{e}_u)_{j-\frac{1}{2}}W_{j-\frac{1}{2}}^+ \\ &= -\epsilon(\hat{e}_q)_{j+\frac{1}{2}}V_{j+\frac{1}{2}}^- + \epsilon(\hat{e}_q)_{j-\frac{1}{2}}V_{j-\frac{1}{2}}^+ - (\hat{e}_u)_{j+\frac{1}{2}}W_{j+\frac{1}{2}}^- + (\hat{e}_u)_{j-\frac{1}{2}}W_{j-\frac{1}{2}}^+, \end{aligned} \quad (3.17)$$

for  $j = n, n+1, \dots, N$ . On the other hand, (3.8) and the properties of the projection operator  $\pi^+$  and  $\pi^-$  imply that

$$\begin{aligned} &B^{(j)}(e_q, e_u; V, W) \\ &= B^{(j)}(e_q, e_u; V - \pi^-V, W - \pi^+W) \\ &= \int_{I_j} (-\epsilon(q - \pi^-q)' + be_q)(V - \pi^-V) dx + \int_{I_j} (-(u - \pi^+u)' + e_q)(W - \pi^+W) dx. \end{aligned} \quad (3.18)$$

By (3.17) and (3.18), we obtain

$$\begin{aligned} &-\epsilon(\hat{e}_q)_{j+\frac{1}{2}}V_{j+\frac{1}{2}}^- + \epsilon(\hat{e}_q)_{j-\frac{1}{2}}V_{j-\frac{1}{2}}^+ - (\hat{e}_u)_{j+\frac{1}{2}}W_{j+\frac{1}{2}}^- + (\hat{e}_u)_{j-\frac{1}{2}}W_{j-\frac{1}{2}}^+ \\ &= \int_{I_j} [-\epsilon(q - \pi^-q)' + be_q](V - \pi^-V) dx + \int_{I_j} [-(u - \pi^+u)' + e_q](W - \pi^+W) dx. \end{aligned} \quad (3.19)$$

Summing up, we have

$$\begin{aligned} &\sum_{j=n}^N \int_{I_j} [-\epsilon(q - \pi^-q)' + be_q](V - \pi^-V) dx + \int_{I_j} [-(u - \pi^+u)' + e_q](W - \pi^+W) dx \\ &= -\epsilon(\hat{e}_q)_{N+\frac{1}{2}}V_{N+\frac{1}{2}}^- + \epsilon(\hat{e}_q)_{n-\frac{1}{2}}(V)_{n-\frac{1}{2}}^+ - (\hat{e}_u)_{N+\frac{1}{2}}(W)_{N+\frac{1}{2}}^- + (\hat{e}_u)_{n-\frac{1}{2}}W_{n-\frac{1}{2}}^+. \end{aligned} \quad (3.20)$$

In terms of  $(\hat{e}_q)_{N+\frac{1}{2}} = 0$ , the adjoint problem (3.15) and its solutions (3.16), (3.20) can be written as

$$\epsilon[(\hat{e}_q)_{n-\frac{1}{2}}]^2 = \sum_{j=n}^N \int_{I_j} [-\epsilon(q - \pi^-q)' + be_q](V - \pi^-V) dx. \quad (3.21)$$

Consequently, we have

$$\begin{aligned}
|(\hat{e}_q)_{n-\frac{1}{2}}|^2 &\leq C(\epsilon) \sum_{j=n}^N (\|(q - \pi^- q)'\|_{I_j} + C_1 \|e_q\|_{I_j}) \|V - \pi^- V\|_{I_j} \\
&\leq C(\epsilon) (h^p |q|_{p+1, \Omega_1} + h^{p+1} \|u\|_{p+2, \Omega}) h^{p+1} |V|_{p+1, \Omega_1} \\
&\leq C(\epsilon) (\|u\|_{p+2, \Omega} + h \|u\|_{p+2, \Omega}) h^{2p+1} |V|_{p+1, \Omega_1}, \tag{3.22}
\end{aligned}$$

where the results of Theorem 3.1 are used. By the expression of (3.16), it is known that

$$\|V\|_{p+1, \Omega_1} \leq C(\epsilon) |(\hat{e}_q)_{n-\frac{1}{2}}|. \tag{3.23}$$

The combination of (3.23) and (3.22) implies that

$$|(\hat{e}_q)_{n-\frac{1}{2}}| \leq C(\epsilon) h^{2p+1} \|u\|_{p+2, \Omega}, \quad n = 1, \dots, N. \tag{3.24}$$

Now we turn to the estimate of  $(\hat{e}_u)_{n+\frac{1}{2}}$ . Consider the adjoint problem in  $[0, x_{n+\frac{1}{2}}]$  with boundary conditions, i.e.,

$$\begin{cases} \epsilon V' + bV + W = 0 & \text{in } \Omega_2 = [0, x_{n+\frac{1}{2}}], \\ W' = 0, \\ V(0) = 0, W(x_{n+\frac{1}{2}}) = (\hat{e}_u)_{n+\frac{1}{2}}, \end{cases} \tag{3.25}$$

which has the solutions (to simplify the notations, we still denote them as  $V$  and  $W$ , resp.)

$$\begin{cases} V = \frac{(\hat{e}_u)_{n+\frac{1}{2}}}{b} (e^{-bx/\epsilon} - 1), \\ W = (\hat{e}_u)_{n+\frac{1}{2}}, \quad \text{in } \Omega_2 = [0, x_{n+\frac{1}{2}}]. \end{cases} \tag{3.26}$$

Obviously (3.19) still holds for  $j = 1, \dots, n$ . Summing up, we have

$$\begin{aligned}
&\sum_{j=1}^n \int_{I_j} [-\epsilon(q - \pi^- q)' + be_q](V - \pi^- V) dx + \sum_{j=1}^n \int_{I_j} [-(u - \pi^+ u)' + e_q](W - \pi^+ W) dx \\
&= -\epsilon(\hat{e}_q)_{n+\frac{1}{2}} V_{n+\frac{1}{2}}^- + \epsilon(\hat{e}_q)_{\frac{1}{2}} (V)_{\frac{1}{2}}^+ - (\hat{e}_u)_{n+\frac{1}{2}} (W)_{n+\frac{1}{2}}^- + (\hat{e}_u)_{\frac{1}{2}} W_{\frac{1}{2}}^+ \\
&= -[(\hat{e}_u)_{n+\frac{1}{2}}]^2 - \epsilon(\hat{e}_q)_{n+\frac{1}{2}} V_{n+\frac{1}{2}}^-, \tag{3.27}
\end{aligned}$$

where  $(\hat{e}_u)_{\frac{1}{2}} = 0$  and the boundary conditions in (3.25) are imposed.

As  $W$  is a constant,  $W - \pi^+ W = 0$ . Similar to (3.22), we get

$$|(\hat{e}_u)_{n+\frac{1}{2}}|^2 \leq \epsilon |(\hat{e}_q)_{n+\frac{1}{2}}| |V_{n+\frac{1}{2}}^-| + C(\epsilon) h^{2p+1} \|u\|_{p+2, \Omega} |V|_{p+1, \Omega_2}. \tag{3.28}$$

In terms of the expression of  $V$  in (3.26), we obtain

$$|V|_{p+1, \Omega_2} \leq C(\epsilon) |(\hat{e}_u)_{n+\frac{1}{2}}|, \quad |V_{n+\frac{1}{2}}^-| \leq C |(\hat{e}_u)_{n+\frac{1}{2}}|.$$

This, combining with (3.28) and (3.24), results in

$$|(\hat{e}_u)_{n+\frac{1}{2}}| \leq C(\epsilon) h^{2p+1} \|u\|_{p+2, \Omega}, \quad n = 1, \dots, N. \tag{3.29}$$

**Corollary 3.3.** *Under the same assumptions as in Theorem 3.1 with  $b = 0$  in (2.1), we have*

$$(\hat{e}_q)_{n-\frac{1}{2}} = 0, \quad (\hat{e}_u)_{n+\frac{1}{2}} = 0, \quad n = 1, 2, \dots, N.$$

*Proof.* When  $b = 0$ , (3.15) has the solutions

$$\begin{cases} V = (\hat{e}_q)_{n-\frac{1}{2}} \\ W = 0, \end{cases}$$

which are constants. So we have  $V - \pi^- V = 0$  in (3.21). Then we get

$$(\hat{e}_q)_{n-\frac{1}{2}} = 0, \quad n = 1, \dots, N. \tag{3.30}$$

On the other hand, (3.25) becomes

$$\begin{cases} \epsilon V' + W = 0 & \text{in } \Omega_2 = [0, x_{n+\frac{1}{2}}], \\ W' = 0, \\ V(0) = 0, W(x_{n+\frac{1}{2}}) = (\hat{e}_u)_{n+\frac{1}{2}}, \end{cases} \quad (3.31)$$

which has the solutions

$$V = -\frac{(\hat{e}_u)_{n+\frac{1}{2}}x}{\epsilon}, \quad W = (\hat{e}_u)_{n+\frac{1}{2}}.$$

For  $p \geq 1$ , we have  $V - \pi^- V = 0$  and  $W - \pi^+ W = 0$ . This fact, combined with (3.27) and (3.30), implies

$$(\hat{e}_u)_{n+\frac{1}{2}} = 0, \quad n = 1, \dots, N.$$

**Remark.** Corollary 3.3 shows that, in the purely elliptic case, the numerical traces capture the exact solution at the nodes of the mesh.

### 4. Numerical Results

The purpose of this section is to demonstrate the superconvergence results of the DG scheme. We consider a test problem under the uniform mesh and modified Shishkin-type meshes with different  $\tau$ , respectively. Denote by  $\|e_u\|_\infty = \|u - \hat{U}\|_\infty$ ,  $\|e_q\|_\infty = \|q - \hat{Q}\|_\infty$ ,  $\|e_u^+\|_\infty = \|u - U^+\|_\infty$  and  $\|e_q^-\|_\infty = \|q - Q^-\|_\infty$ , the errors in the maximum norm at nodal points.

Consider the equation

$$\begin{cases} -\epsilon u'' + u' = e^x & \text{in } (0, 1), \\ u(0) = 0, \\ u'(1) = \frac{\epsilon e(1-e^{-\frac{1}{\epsilon}})+1-e}{\epsilon(1-\epsilon)(1-e^{-\frac{1}{\epsilon}})}, \text{ when } \epsilon \neq 1, \\ u'(1) = \frac{e(2-e)}{e-1}, \text{ when } \epsilon = 1, \end{cases} \quad (4.1)$$

with the exact solution

$$u = \begin{cases} \frac{e^x(1-e^{-\frac{1}{\epsilon}})+e^{1-\frac{1}{\epsilon}}-1+(1-\epsilon)e^{\frac{x-1}{\epsilon}}}{(1-\epsilon)(1-e^{-\frac{1}{\epsilon}})} & \epsilon \neq 1 \\ \frac{e}{e-1}(e^x - 1) - xe^x & \epsilon = 1, \end{cases} \quad (4.2)$$

which exhibits a boundary layer with the order of magnitude  $O(\epsilon)$ , at the outflow boundary  $x = 1$ .

Listed in Tables 4.1-4.2 are the errors in the maximum norm at nodal points and the corresponding convergence rates of the DG solutions for (4.1) under the uniform mesh with  $\epsilon = 10^{-1}$  and  $\epsilon = 10^{-2}$ , respectively. The first column shows the degree  $p$  of the polynomial we used to approximate the unknown  $u$  and  $q$ . The second column is the mesh number, where  $i = 5, 6, \dots, 9$  indicates a uniform mesh with  $2^i$  evenly distributed elements.

When  $\epsilon$  is small, we failed to maintain the reasonable superconvergence rates numerically. Plotted in Fig. 4.1 and Fig. 4.2 are the convergence curves of the numerical traces for (4.1) in the maximum norm at nodal points for  $\epsilon = 1$ ,  $\epsilon = 10^{-1}$ , and  $\epsilon = 10^{-2}$  with  $p = 1$ . Though the  $2p + 1$  superconvergence order is observed, the error bound is strongly dependent on  $\epsilon$ . Plotted in Figs. 4.3-4.6 are the figures of the exact solution  $u$ , the numerical trace  $\hat{U}$ , the exact derivative  $u'$  and the numerical trace  $\hat{Q}$  at the nodes with  $\epsilon = 10^{-2}$  and  $\epsilon = 10^{-10}$ , respectively. Obviously, these figures show that the DG solutions do not have any oscillatory behavior even for small  $\epsilon$ . In other words, the DG method is more “local” than the traditional finite element method.

Table 4.1: Numerical results of (4.1), uniform mesh,  $\epsilon = 0.1$ 

p	mesh	$\hat{e}_u$		$e_u^+$		$e_q^-$		$\hat{e}_q$	
		error	order	error	order	error	order	error	order
1	5	2.75e-04	2.88	2.51e-02	1.74	1.87e-01	1.32	2.75e-03	2.88
	6	3.56e-05	2.95	6.90e-03	1.86	6.00e-02	1.64	3.56e-04	2.95
	7	4.55e-06	2.97	1.81e-03	1.93	1.70e-02	1.82	4.55e-05	2.97
	8	5.74e-07	2.99	4.66e-04	1.96	4.54e-03	1.91	5.74e-06	2.99
	9	7.22e-08	2.99	1.18e-04	1.98	1.17e-03	1.95	7.21e-07	2.99
2	5	2.76e-07	4.90	8.06e-04	2.74	5.90e-03	2.29	2.76e-06	4.91
	6	8.83e-09	4.97	1.10e-04	2.87	9.46e-04	2.64	8.83e-08	4.97
	7	2.78e-10	4.98	1.45e-05	2.93	1.34e-04	2.82	2.80e-09	4.98
	8	1.33e-11	4.39	1.85e-06	2.97	1.78e-05	2.91	9.10e-11	4.94
	9	2.94e-11	-	2.34e-07	2.98	2.30e-06	2.95	5.08e-11	-
3	5	1.39e-10	6.92	1.81e-05	3.75	1.33e-004	3.30	1.39e-009	6.92
	6	9.97e-13	7.12	1.24e-06	3.87	1.06e-005	3.65	1.11e-011	6.97
	7	1.13e-12	-	8.10e-08	3.94	7.49e-007	3.82	2.97e-012	-
	8	6.90e-12	-	5.17e-09	3.97	4.98e-008	3.91	1.68e-011	-
	9	6.88e-12	-	3.20e-10	4.01	3.21e-009	3.96	1.62e-011	-

Table 4.2: Numerical results of (4.1), uniform mesh,  $\epsilon = 0.01$ 

p	mesh	$\hat{e}_u$		$e_u^+$		$e_q^-$		$\hat{e}_q$	
		error	order	error	order	error	order	error	order
1	6	2.42e-02	1.92	3.12e-01	1.14	8.06e+00	-	2.42e+00	1.92
	7	3.51e-03	2.78	1.12e-01	1.48	5.31e+00	-	3.51e-01	2.78
	8	4.76e-04	2.88	3.47e-02	1.70	2.36e+00	1.17	4.76e-02	2.88
	9	6.29e-05	2.92	9.73e-03	1.83	8.01e-00	1.56	6.29e-03	2.92
	10	8.05e-06	2.97	2.59e-03	1.91	2.35e-01	1.77	8.05e-04	2.97
2	6	6.30e-04	3.84	4.72e-002	2.01	9.16e-01	-	6.30e-02	3.84
	7	2.26e-05	4.80	8.82e-003	2.42	4.00e-01	1.19	2.26e-03	4.80
	8	7.50e-07	4.91	1.37e-003	2.69	9.27e-02	2.11	7.50e-05	4.91
	9	2.44e-08	4.94	1.92e-004	2.84	1.58e-02	2.55	2.44e-06	4.94
	10	7.73e-10	4.98	2.54e-005	2.92	2.30e-03	2.78	7.75e-08	4.98
3	6	8.14e-06	5.81	5.31e-03	2.94	1.12e-01	-	8.14e-04	5.81
	7	7.22e-08	6.82	4.99e-04	3.41	2.28e-02	2.29	7.22e-06	6.82
	8	5.92e-10	6.93	3.86e-05	3.69	2.61e-03	3.13	5.93e-08	6.93
	9	4.54e-12	7.03	2.69e-06	3.84	2.21e-04	3.56	4.79e-10	6.95
	10	2.16e-11	-	1.78e-07	3.92	1.61e-05	3.78	6.07e-011	-

Now we turn to the DG method based on the Shishkin mesh. The construction of the so-called Shishkin mesh is as follows:

First choose a positive  $\tau < \frac{1}{2}$ . In our experience, one can choose  $\tau$  to match the length of the boundary layer, e.g.,  $O(\epsilon)$  in our test problem. Next the intervals  $(0, 1 - \tau)$  and  $(1 - \tau, 1)$  are each divided into  $N_1$  equal subintervals. As a result, the number of cells of the Shishkin mesh is  $N = 2N_1$ .

We take  $\tau = (2p+1)\epsilon \ln(N+1)$  first. Listed in Tables 4.3-4.4 are the errors in the maximum norm of the numerical traces at nodal points and the corresponding convergence rates with  $p = 1, p = 2$  for  $\epsilon = 10^{-2}$  and  $\epsilon = 10^{-5}$ , respectively. The first column in the tables is the mesh number in  $[0, 1 - \tau]$  and  $[1 - \tau, 1]$ , where  $i$  means we used a  $2^i$  evenly distributed elements

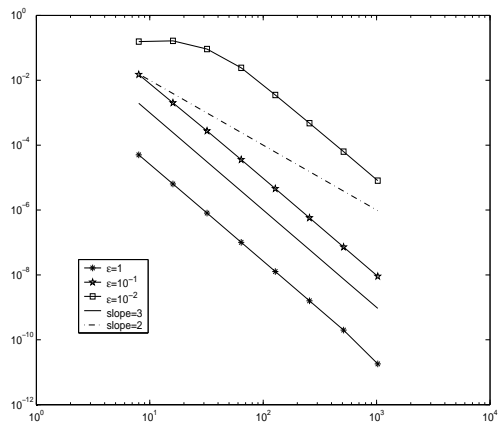


Fig. 4.1. Convergence curve of  $\hat{U}$  for (4.1), the uniform mesh,  $p = 1$

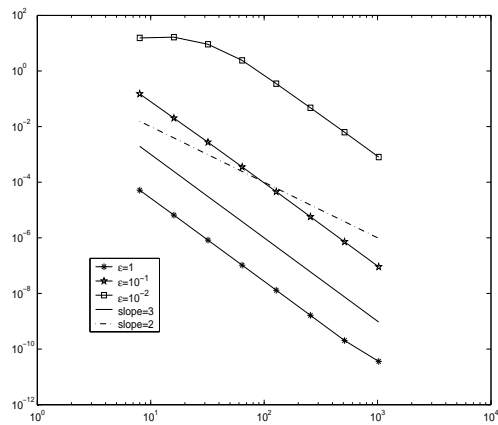


Fig. 4.2. Convergence curve of  $\hat{Q}$  of (4.1), the uniform mesh,  $p = 1$

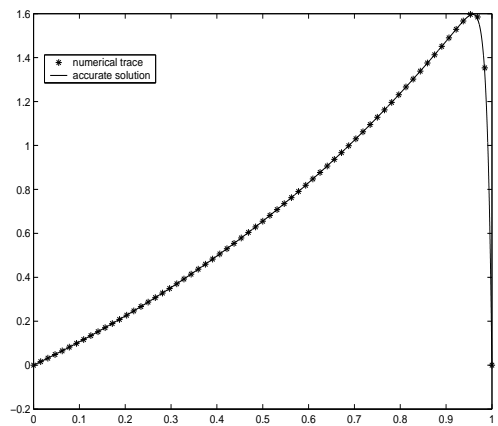


Fig. 4.3.  $u$  and  $\hat{U}$  of (4.1),  $\epsilon = 10^{-2}$ ,  $p = 1$ ,  $N = 64$

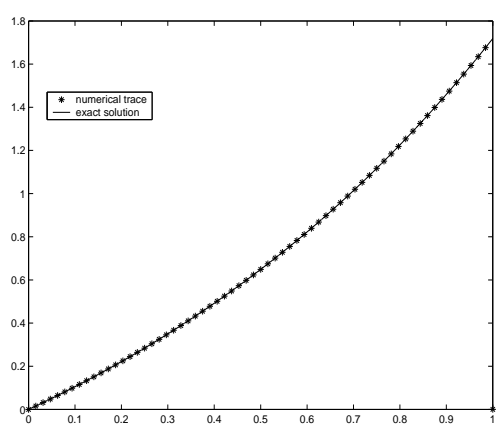


Fig. 4.4.  $u$  and  $\hat{U}$  of (4.1),  $\epsilon = 10^{-10}$ ,  $p = 1$ ,  $N = 64$

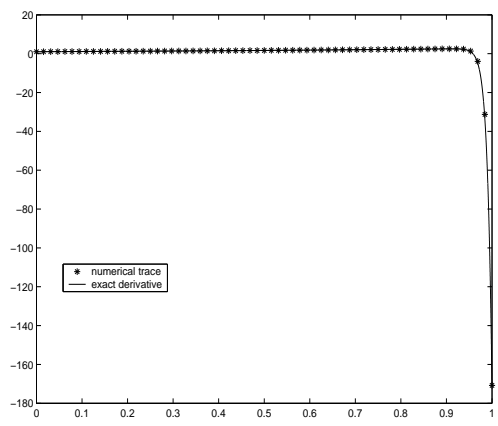


Fig. 4.5.  $u'$  and  $\hat{Q}$  of (4.1),  $\epsilon = 10^{-2}$ ,  $p = 1$ ,  $N = 64$

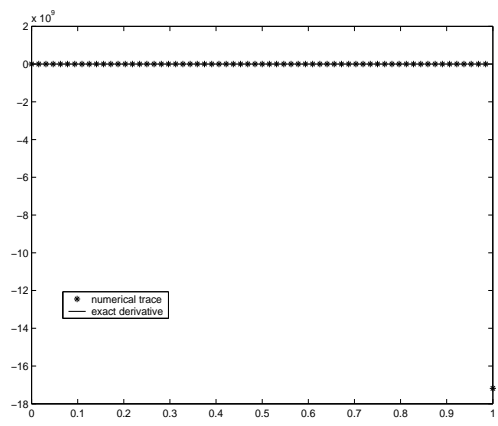


Fig. 4.6.  $u'$  and  $\hat{Q}$  of (4.1),  $\epsilon = 10^{-10}$ ,  $p = 1$ ,  $N = 64$

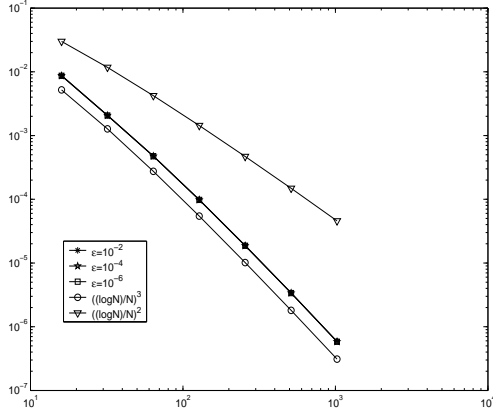


Fig. 4.7. Convergence curve of  $\hat{e}_u$  for (4.1), Shishkin mesh,  $\tau = (2p + 1)\epsilon \ln(N + 1)$ ,  $p = 1$

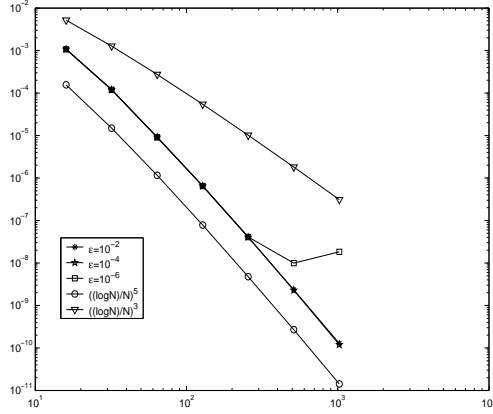


Fig. 4.8. Same as Fig. 4.7, except  $p = 2$

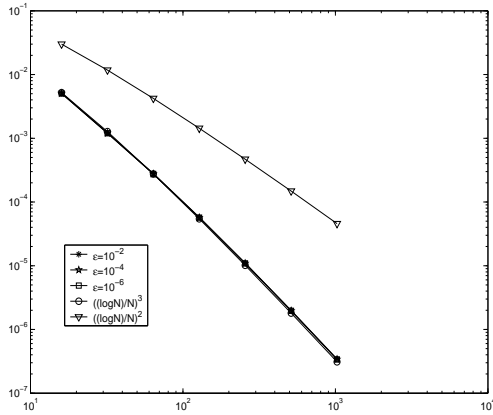


Fig. 4.9. Convergence curve of  $\hat{e}_q$  for (4.1), Shishkin mesh,  $\tau = (2p + 1)\epsilon \ln(N + 1)$ ,  $p = 1$

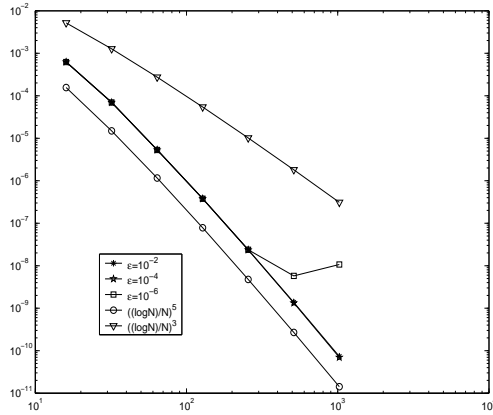


Fig. 4.10. Same as Fig. 4.9, except  $p = 2$

in  $[0, 1 - \tau]$  and  $[1 - \tau, 1]$ , respectively. Plotted in Figs. 4.7-4.10 are the convergence curves of the numerical traces for (4.1) in the maximum norm at nodal points for  $\epsilon = 10^{-2}$ ,  $\epsilon = 10^{-4}$  and  $\epsilon = 10^{-6}$  with  $p = 1, p = 2$ , respectively. As the derivative  $u'$  becomes very large in the boundary layer when  $\epsilon$  is small, instead of the absolute error, the error in terms of  $Q$  in Tables 4.3-4.6, Figs. 4.9-4.10 and Figs. 4.13-4.14 is the relative one, i.e.,  $\frac{\|u' - Q\|_\infty}{\|u'\|_\infty}$ .

The numerical results in Tables 4.3-4.4 and Figs. 4.7-4.10 imply that the DG solutions have the error estimates

$$\|\hat{e}_u\|_\infty \leq C\left(\frac{\ln N}{N}\right)^{2p+1}, \quad \|\hat{e}_q\|_\infty \leq C\left(\frac{\ln N}{N}\right)^{2p+1}|u|_{1,\infty} \quad (4.3)$$

for Shishkin mesh with  $\tau = (2p + 1)\epsilon \ln(N + 1)$ , where  $C$  is independent of  $\epsilon$ .

Now we consider the DG method based on the Shishkin mesh with  $\tau = -(2p + 1)\epsilon \ln \epsilon$ . Listed in Tables 4.5-4.6 are the errors in the maximum norm at nodal points and the corresponding convergence rates for  $p = 1, p = 2$  with  $\epsilon = 10^{-2}$ ,  $\epsilon = 10^{-4}$ , and  $\epsilon = 10^{-6}$ , respectively. Plotted in Figs. 4.11-4.14 are the convergence curves of numerical traces for (4.1) in the maximum norm at nodal points for  $\epsilon = 10^{-2}$ ,  $\epsilon = 10^{-4}$  and  $\epsilon = 10^{-6}$  with  $p = 1, p = 2$ , respectively.

The numerical results in Tables 4.5-4.6 and Figs. 4.11-4.14 show that, though the errors seem to depend on  $\epsilon$ , the bound of the errors is independent of  $\epsilon$  at all. So we have the following

Table 4.3:  $\hat{e}_u$  and  $\hat{e}_q$  for (4.1),  $\tau = (2p + 1)\epsilon \ln(N + 1)$ ,  $p = 1, p = 2$ ,  $\epsilon = 10^{-2}$

mesh	$p = 1$				$p = 2$			
	$\hat{e}_u$		$\hat{e}_q$		$\hat{e}_u$		$\hat{e}_q$	
	error	order	error	order	error	order	error	order
5	4.78e-04	2.12	1.22e-03	2.07	9.18e-06	3.71	7.06e-05	3.16
6	9.87e-05	2.28	2.80e-04	2.12	6.54e-07	3.81	5.38e-06	3.71
7	1.89e-05	2.39	5.77e-05	2.28	4.08e-08	4.00	3.83e-07	3.81
8	3.40e-06	2.47	1.10e-05	2.39	2.34e-09	4.13	2.39e-08	4.00
9	5.88e-07	2.53	1.99e-06	2.47	1.29e-10	4.18	1.37e-09	4.13

Table 4.4:  $\hat{e}_u$  and  $\hat{e}_q$  for (4.1),  $\tau = (2p + 1)\epsilon \ln(N + 1)$ ,  $p = 1, p = 2$ ,  $\epsilon = 10^{-5}$

mesh	$p = 1$				$p = 2$			
	$\hat{e}_u$		$\hat{e}_q$		$\hat{e}_u$		$\hat{e}_q$	
	error	order	error	order	error	order	error	order
5	4.73e-004	2.12	1.20e-03	2.07	9.09e-06	3.71	6.95e-05	3.16
6	9.77e-005	2.28	2.75e-04	2.12	6.48e-07	3.81	5.29e-06	3.71
7	1.87e-005	2.39	5.68e-05	2.28	4.04e-08	4.00	3.77e-07	3.81
8	3.37e-006	2.47	1.09e-05	2.39	2.00e-09	4.34	2.35e-08	4.00
9	5.83e-007	2.53	1.96e-06	2.47	2.33e-09	-	1.16e-09	4.34

Table 4.5:  $\hat{e}_u$  and  $\hat{e}_q$  for (4.1),  $\tau = -(2p + 1)\epsilon \ln \epsilon$ ,  $p = 1, p = 2$ ,  $\epsilon = 10^{-2}$

mesh	$p = 1$				$p = 2$			
	$\hat{e}_u$		$\hat{e}_q$		$\hat{e}_u$		$\hat{e}_q$	
	error	order	error	order	error	order	error	order
5	6.39e-04	2.90	2.79e-03	2.68	1.48e-05	4.89	2.56e-04	3.98
6	8.41e-05	2.92	3.74e-04	2.90	5.04e-07	4.87	8.64e-06	4.89
7	1.08e-05	2.96	4.93e-05	2.92	1.62e-08	4.96	2.95e-07	4.87
8	1.37e-06	2.98	6.35e-06	2.96	1.62e-08	4.96	9.47e-09	4.96
9	1.73e-07	2.99	8.04e-07	2.98	2.06e-11	4.64	3.01e-10	4.97

Table 4.6:  $\hat{e}_u$  and  $\hat{e}_q$  for (4.1),  $\tau = -(2p + 1)\epsilon \ln \epsilon$ ,  $p = 1, p = 2$ ,  $\epsilon = 10^{-5}$

mesh	$p = 1$				$p = 2$			
	$\hat{e}_u$		$\hat{e}_q$		$\hat{e}_u$		$\hat{e}_q$	
	error	order	error	order	error	order	error	order
5	9.07e-03	2.42	2.82e-02	1.43	1.14e-03	3.59	8.03e-03	2.17
6	1.22e-03	2.90	5.28e-03	2.42	4.57e-05	4.64	6.65e-04	3.59
7	1.61e-04	2.92	7.09e-04	2.90	1.50e-06	4.93	2.66e-05	4.64
8	2.08e-05	2.95	9.37e-05	2.92	4.79e-08	4.97	8.74e-07	4.93
9	2.65e-06	2.97	1.21e-05	2.95	1.35e-09	5.15	2.79e-08	4.97

error estimates,

$$\|\hat{e}_u\|_\infty \leq CN^{-(2p+1)}, \quad \|\hat{e}_q\|_\infty \leq CN^{-(2p+1)}|u|_{1,\infty}, \quad (4.4)$$

for the Shishkin mesh with  $\tau = -(2p + 1)\epsilon \ln \epsilon$ .

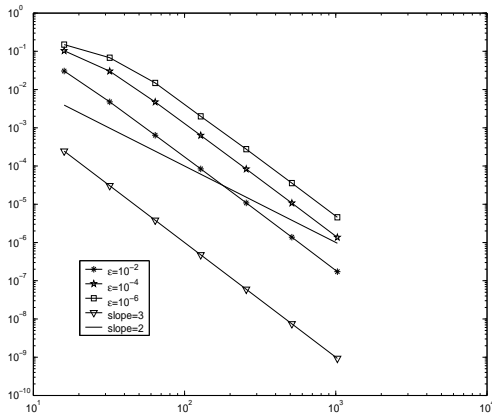


Fig. 4.11. Convergence curve of  $\hat{e}_u$  for (4.1), Shishkin mesh,  $\tau = -(2p + 1)\epsilon \ln \epsilon$ ,  $p = 1$

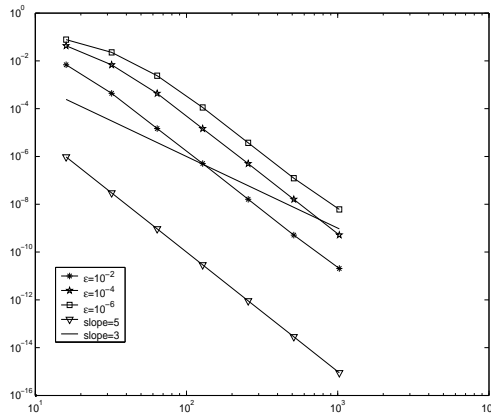


Fig. 4.12. Same as Fig. 4.11, except  $p = 2$

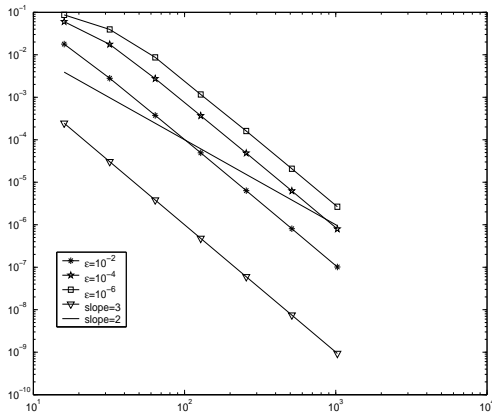


Fig. 4.13. Convergence curve of  $\hat{e}_q$  for (4.1), Shishkin mesh,  $\tau = -(2p + 1)\epsilon \ln \epsilon$ ,  $p = 1$

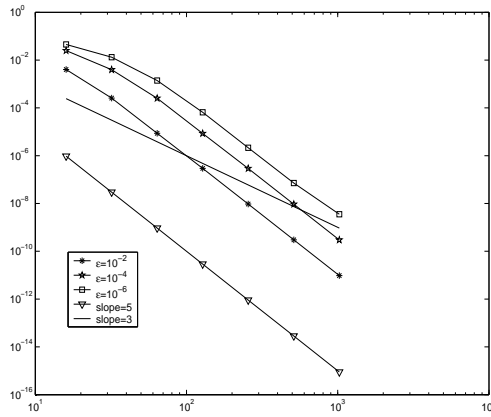


Fig. 4.14. Same as Fig. 4.13, except  $p = 2$

### 5. Conclusion

In this article, motivated by DG methods for hyperbolic equations, we designed a DG scheme to solve the singularly-perturbed convection-diffusion equations in the one-dimensional setting. The verification of the existence and uniqueness of the approximate solution is provided. Further, we have established the  $2p + 1$ -order superconvergence properties of the DG scheme. Our numerical results show that the DG method does not produce any oscillation even under the uniform mesh. In other words, the DG method is more “local” than the traditional finite element method. This is a very fantastic property. The mathematical reason behind is an ongoing work. Our numerical results demonstrate that, under the uniform mesh, it seems impossible to obtain the uniform superconvergence of the numerical traces. Nevertheless, thanks to the implementation of the so-called Shishkin-type mesh with an appropriately chosen  $\tau$ , the uniform  $2p + 1$ -order superconvergence is observed in our numerical experiments. The theoretical verification of this phenomenon is our future work.

Our research shows that the combination of DG methods and the anisotropic meshes is one of the most robust approaches in the study of the numerical methods for singularly perturbed problems.

**Acknowledgments.** The first version of this work was done when the first author visited Wayne State University (WSU). The support of the Department of Mathematics at WSU is greatly appreciated.

## References

- [1] D.N. Arnold, F. Brezzi, B. Cockburn and L.D. Marini, Unified analysis of discontinuous Galerkin methods for elliptic problems, *SIAM J. Numer. Anal.*, **39** (2002), 1749-1779.
- [2] A. Buffa, T.J.R. Hughes, and G. Sangalli, Analysis of a multiscale discontinuous Galerkin method for convection-diffusion problems, *SIAM J. Numer. Anal.*, **44** (2006), 1420-1440.
- [3] F. Celiker and B. Cockburn, Superconvergence of the numerical traces of discontinuous Galerkin and Hybridized methods for convection-diffusion problems in one space dimension, *Math. Comp.*, **76** (2007), 67-96.
- [4] C.M. Chen, Structure Theory of Superconvergence of Finite Elements (in Chinese), Hunan Science Press, P.R. China, 2001.
- [5] C. Chen and Y. Huang, High Accuracy Theory of Finite Element Methods (in Chinese), Hunan Science Press, China, 1995.
- [6] Z. Chen and G. Ji, Sharp  $L^1$  a posteriori error analysis for nonlinear convection-diffusion problems, *Math. Comp.*, **75** (2006), 43-71.
- [7] B. Cockburn, G.E. Karniadakis, and C.-W. Shu, The development of discontinuous Galerkin methods, in Discontinuous Galerkin Methods, Theory, Computation and Applications, B. Cockburn, G.E. Karniadakis, and C.-W. Shu, eds., Lecture Notes in Comput. Sci. Engrg. 11, Springer-Verlag, New York, 2000.
- [8] B. Cockburn and C.-W. Shu, The local discontinuous Galerkin method for time-dependent convection-diffusion systems, *SIAM J. Numer. Anal.*, **35** (1998), 2440-2463.
- [9] M. Křížek, P. Neittaanmäki, and R. Stenberg (Eds.), Finite Element Methods: Superconvergence, Post-processing, and A Posteriori Estimates, Lecture Notes in Pure and Applied Mathematics, Vol. 196, Marcel Dekker, Inc., New York, 1998.
- [10] D. Leykekhman, Uniform error estimates in the finite element method for a singularly perturbed reaction-diffusion problem, *Math. Comp.*, to appear.
- [11] Q. Lin and N. Yan, Construction and Analysis of High Efficient Finite Elements (in Chinese), Hebei University Press, P.R. China, 1996.
- [12] T. Linß, Robustness of an upwind finite difference scheme for semilinear convection-diffusion problems with boundary turning points, *J. Comp. Math.*, **21** (2003), 401-410.
- [13] W.-B. Liu and T. Tang, Error analysis for a Galerkin-spectral method with coordinate transformation for solving singularly perturbed problems, *Appl. Numer. Math.*, **38** (2001), 315-345.
- [14] J.J. Miller, E. O'Riordan, and G.I. Shishkin, Fitted Numerical Methods for Singular Perturbation Problems, World Scientific, Singapore, 1996.
- [15] K.W. Morton, Numerical Solution of Convection-Diffusion Problems, Chapman and Hall, London, 1996.
- [16] W.H. Reed and T.R. Hill, Trigngular mesh methods for the neutron transport equation, Tech. Report LA-UR-73-479, Los Alamos Scientific Laboratory, Los, Alamos, NM, 1973.
- [17] H.-G. Roos, Layer-adapted grids for singular perturbation problems, *ZAMM Z. Angew. Math. Mech.*, **78** (1998), 291-309.
- [18] H.-G. Roos, M. Stynes, and L. Tobiska, Numerical Methods for Singularly Perturbed Differential Equations, Springer, Berlin, 1996.
- [19] G. Sangalli, Robust a-posteriori estimator for advection-diffusion-reaction problems, *Math. Comp.*, to appear.
- [20] G.I. Shishkin, Discrete approximation of singularly perturbed elliptic and parabolic problems (in Russian), Russian Academy of Sciences, Ural Section, Ekaterinburg, 1992.

- [21] C. Schwab and M. Suri, The  $p$  and  $hp$  versions of the finite element method for problems with boundary layers, *Math. Comp.*, **65** (1996), 1403-1429.
- [22] M. Stynes, Steady-state convection-diffusion problems, in *Acta Numerica 2005* (A. Iserles, ed.), Cambridge University Press, Cambridge, 445-508.
- [23] L.B. Wahlbin, Superconvergence in Galerkin Finite Element Methods, *Lecture Notes in Mathematics*, Vol. 1605, Springer, Berlin, 1995.
- [24] Y. Xu and C.-W. Shu, Local discontinuous Galerkin methods for three classes of nonlinear wave equations. *J. Comp. Math.*, **22** (2004), 250-274.
- [25] Z. Zhang, On the  $hp$  finite element method for the one dimensional singularly perturbed convection-diffusion problems. *J. Comp. Math.*, **20** (2002), 599-610.
- [26] Z. Zhang, Finite element superconvergent approximation for one-dimensional singularly perturbed problems, *Numer. Meths. PDEs.*, **18** (2002), 374-395.
- [27] Q.D. Zhu and Q. Lin, *Superconvergence Theory of the Finite Element Method* (in Chinese), Hunan Science Press, China, 1989.